

Electronic Structure and Properties of the Organic Semi Conductor Material Anthracene in Gas Phase and Ethanol: An ab Initio and DFT Study

Umar Gurku¹ and Chifu E. Ndikilar^{2,*}

¹Physics Department, Nasarawa State University, Keffi, Nigeria

²Physics Department, Federal University Dutse, Dutse, Jigawa State, Nigeria

The molecular geometry of Anthracene in gas phase and ethanol are studied using ab initio quantum chemical calculations at the Restricted Hartree-Fock (RHF) level of theory by employing 6-31G basis set. Density functional calculations at the Becke3LYP (B3LYP) are carried out using 6-31G basis set for inclusion of electron correlations. The molecular structure, dipole moment, quadrupole moment, charge transfer, polarizability, energy, and vibrational frequencies with IR and Raman intensities have been studied. At both levels of theory, it is predicted that the solvent (ethanol) has an effect of expanding the molecule as there is a slight increase in most of the bond lengths, bond angles and dihedral angles. The predicted dipole moment for Anthracene is almost zero at RHF/6-31G level and zero at B3LYP/6-31G level indicating that the molecule is not polar and the charge distribution is fairly symmetrical. The quadrupole moment predicts that the molecule is slightly elongated along the ZZ axis. Using the total energies, it is predicted that the molecule is slightly more stable in gas phase than in ethanol. The change in polarizability tensors is found to be more pronounced in solution than in the gas phase.

1. Introduction

With the advent of modern physics, new fundamental types of materials have been created. Various types of forces operating in different classes of solids are exploited in the design of molecular materials. A variety of fabrication techniques have been developed with the desired properties. The quest for more efficient and cheaper materials for use in industry has led to the discovery of molecular materials. An organic semiconductor is an organic material with semiconductor properties. Single molecule, short chain and organic polymers can be semi conductive. Semiconducting small molecules include the polycyclic aromatic compound, pentacene, anthracene and rubrene. Polymeric organic semiconductors include, poly(3-hexylthiophene), poly(p-phenylene vinylene), as well as polyacetylene and its derivatives. Typical current carriers in organic semiconductors are holes and electrons in π bonds. Almost all organic solids are insulators, but when their constituent molecules have π conjugate systems, electrons can move via π -electron cloud overlaps, especially by hopping, tunneling and related mechanisms [1].

This work examines the molecular and electronic properties of an organic semi conductor material anthracene. Anthracene has molecular

Formula $C_{14}H_{10}$ with a molar mass of 178.23g mol^{-1} . It is soluble in alcohols, benzene, hydronaphthalenes, carbon disulfide, chloroform, and other organic solvents. Anthracene is a solid polycyclic aromatic compound consisting of three fused benzene rings. It is a component of coal-tar. Anthracene is also used in the production of red dye alizarin and other dyes. Anthracene is colorless but exhibits a blue (400-500 nm peak) fluorescence under ultraviolet light [2].

Here, the windows version of Gaussian software is used to predict the molecular energies and structures, atomic charges and electrostatic potentials, vibrational frequencies, IR and Raman spectra, and polarizabilities of anthracene.

2. Computational Methodology

2.1. Gaussian package

The Gaussian package is a computational physics and chemistry program. The name comes from the fact that it uses Gaussian type basis functions. It is used for electronic and geometric structure optimization (single point calculation, geometry optimization, transition states, and reaction path modeling), and molecular properties and vibrational analysis (IR, Raman, NMR vibrational frequencies and normal modes, electrostatic potential, electron density, multi-pole moments, population analysis, natural orbital analysis, magnetic shielding induced current densities, static

*ebenechifu@yahoo.com

and frequency-dependent polarizabilities, and hyperpolarizabilities) using both DFT and ab initio methods.

2.2. Geometry and vibrational frequency optimization

Geometry optimization is done by locating both the minima and transition states on the potential surface of the molecular orbital. It can be optimized in Cartesian coordinates that are generated automatically from the input Cartesian coordinates. It also handles fixed constraints on distances, bond angles and dihedral angles in Cartesian or (where appropriate) internal coordinates. The process is iterative, with repeated calculations of energies and gradients and calculations or estimations of Hessian in every optimization cycle until convergence is attained

One of the most computationally demanding aspects of calculating free energy using electronic structure theory is the calculation of vibrational energy and entropy contributions. The computational expense is incurred by the calculation of the matrix of second energy-derivatives (i.e., the Hessian or force constant matrix), which yields harmonic vibrational frequencies upon diagonalization.

2.3. Computation of molecular properties

The molecular structures and geometries of the organic semiconductor material anthracene is completely optimized using ab initio quantum mechanical calculations at the Restricted Hartree-Fock (RHF) level of theory without using any symmetry constraints. Geometry optimizations are performed using the ab initio RHF method with 6-31G basis set. The structures are refined further using Density Functional Theory, which is a cost effective method for inclusion of electron correlations with the three-parameter density functional generally known as Becke3LYP (B3LYP) [3]. At the first step, geometry optimizations are carried out then, the IR and Raman frequencies are calculated using the Hessian, which is the matrix of second derivatives of the energy with respect to geometry.

Since the gas phase results are inadequate for describing the behavior of molecules in solutions we therefore investigate the effect of solvating the molecule in bulk in ethanol. For this purpose, the simplest Onsager reaction field model of the self-consistent reaction field (SCRf) theory is used with the 6-31G basis set. In this calculation, the solute occupies a fixed spherical cavity within the solvent

field. The electric dipole of the solute molecule induces a dipole in the medium and the electric field applied by the induced solvent dipole interacts with the molecular dipole and affects it.

3. Results and Discussion

3.1. Optimized molecular structure

Geometry optimizations usually attempt to locate minima on the potential energy surface, thereby predicting equilibrium structures of molecular systems [4]. At the minima, the first derivative of the energy (gradient) is zero. Since the gradient is the negative of the forces, the forces are also zero at such a point (stationary point). In Gaussian, a geometry optimization begins at the molecular structure specified at the input and steps along the potential energy surface. It computes the energy and the gradient at that point and determines which direction to make the next step. The gradient indicates the direction along the surface in which the energy decreases most rapidly from the current point as well as the steepness of that slope. The optimized parameters are the bond lengths (in Armstrong), the bond angles and the dihedral angles for the optimized molecular structure. Atoms in the molecule are numbered according to their order in the molecule specification section of the input.

The optimized bond lengths of Anthracene in gas phase, methanol and ethanol are listed in Table 1. The optimized molecular structure is shown in Fig. 1. The predicted bond lengths at RHF/6-31G level in gas phase are slightly smaller than the corresponding values in ethanol and the same is obtained at the DFT/B3LYP/6-31G level of theory. Changes in bond lengths are noticed when one goes from the RHF/6-31G to B3LYP/6-31G level, but no significant change in the bond angles is noticed in the gas phase. It seems inclusion of electron correlation expands the molecule. The bond angles and dihedral angles on the other hand remain largely unaffected by the solvent (Tables 2 and 3) except for some few cases where the orientation of dihedral angles changes.

3.2. Dipole moments, quadrupole moments and energies

The dipole moment is the first derivative of the energy with respect to an applied electric field. It is a measure of the asymmetry in the molecular charge distribution and is given as a vector in three dimensions. For Hartree-Fock calculations, this is equivalent to the expectation values of X, Y and Z,

which are the quantities reported in the output. The predicted dipole moments (in Debye) at different levels of theory are shown in Table 4. The dipole moment of the molecules gives the strength of the polarity of the molecule. The predicted dipole moment is almost zero at RHF/6-31G level and zero at B3LYP/6-31G level. Thus, the molecule is non polar and the charge distribution is fairly symmetrical.

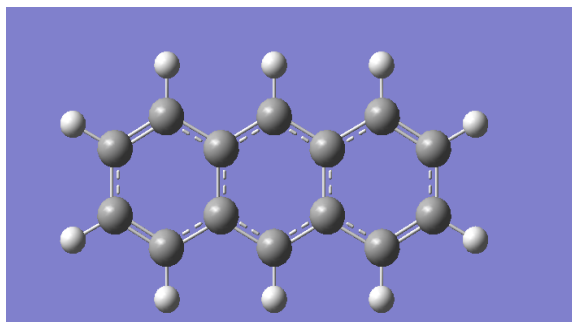


Fig.1: Optimized structure of anthracene.

Quadrupole moments provide a second order approximation of the total electron distribution, providing at least a crude idea of its shape. One of the components being significantly larger than the others would represent an elongation of the sphere along that axis. If present, the off-axis components represent trans-axial distortion (stretching or compressing of the ellipsoid). The quadrupole moment for the molecule at different levels of theory is shown in Table 5. The molecule is predicted to be slightly elongated along the ZZ axis and this elongation increases in ethanol at the RHF/6-31G and B3LYP/6-31G levels.

All frequency calculations include thermochemical analysis of the molecular system. By default, this analysis is carried out at 298.15 K and 1 atmosphere of pressure, using the principal isotope of each element type in the molecular system. Predicted total, electronic, translational, rotational and vibrational energies in kcal/mol for the molecule both in gas phase and in ethanol is listed on Table 6. The translational energy relates to the displacement of molecules in space as a function of the normal thermal motions of matter. Rotational energy is observed as the tumbling motion of a molecule as a result of the absorption of energy within the microwave region. The vibrational energy component is a higher energy term and corresponds to the absorption of energy by a molecule as the component atoms vibrate about the mean center of their chemical bonds. The electronic component is linked to the energy

transitions of electrons as they are distributed throughout the molecule, either localized within specific bonds, or delocalized over structures, such as an aromatic ring.

It is seen that the molecule is slightly more stable in gas phase. The difference in total energies from gaseous to ethanol is a bit larger when electron correlation is included. Anthracene is found to be the most stable, approximately by 2.20 kcal/mol at RHF/6-31G level and by nearly 0.1 kcal/mol at B3LYP/6-31G in gas phase as compared to ethanol. This shows that the presence of ethanol tends to reduce its stability that may be of importance in its effectiveness in use.

3.3. Charge transfer and polarizabilities

Within molecular system, atoms can be treated as a quantum mechanical system. On the basis of the topology of the electron density the atomic charges in the molecule can be explained. The electrostatic potential derived charges using the CHelpG scheme of Breneman at different atomic positions in gas phase and in ethanol of Anthracene at RHF/6-31G and B3LYP/6-31G levels of theories is given in Table 7. The Mulliken population analysis partitions the charges among the atoms of the molecule by dividing orbital overlap evenly between two atoms. Whereas the electrostatic potential derived charges assign point charges to fit the computed electrostatic potential at a number of points on or near the Van der Waal surface. Hence, it is appropriate to consider the charges calculated by CHelpG scheme of Breneman instead of Mulliken population analysis.

It is clear from Table 7 that the amount of charges on C2, C3, C4, C6, C7, C8, C10, C11, C15, H16 and H21 atoms increases, while on C1, C5, C9, H12, C13, C14, H17, H18, H19, H20, H22, H23 and H24 atoms decreases at RHF/6-31G level and at B3LYP/6-31G level decreases in ethanol than that of gas phase charges. It means that former atoms acquire charges from the solvent medium while later atoms loses their charges to the solvent medium due to the effect of the solvent.

Polarizability refers to the way the electrons around an atom redistribute themselves in response to an electrical disturbance. The polarizability tensor components of anthracene molecule in gas phase as well as in ethanol obtained at RHF/6-31+G and B3LYP/6-31+G levels of theory is listed on Table 8. The polarizability tensor components of anthracene molecule show a change in going from gas phase to solution at both levels of theory. All the six polarizability tensor components (xx,

xy, yy, xz, yz and zz) of anthracene molecule increases significantly at both levels of theory, but they do not follow any regular pattern. The change in polarizability tensors is more pronounced in ethanol than in the gas phase. This may be due to the fact that the polarity of the solvent (ethanol)

and the dipole moments of the molecule are more in ethanol than in the gas phase.

Table 1: Optimized bond lengths (\AA) of anthracene molecule.

Geometrical Parameter	RHF/6-31G	B3LYP/6-31		
	Gas	Ethanol	Gas	Ethanol
R(1,2)	1.3466	1.3546	1.3739	1.3754
R(1,6)	1.4299	1.4313	1.4288	1.4306
R(1,17)	1.0719	1.0751	1.0854	1.0877
R(2,3)	1.4341	1.4358	1.4329	1.4344
R(2,18)	1.0729	1.0762	1.0864	1.0887
R(3,4)	1.4245	1.4289	1.4491	1.4503
R(3,7)	1.3874	1.3929	1.4036	1.4051
R(4,5)	1.4341	1.4358	1.4329	1.4344
R(4,8)	1.3874	1.3929	1.4036	1.4051
R(5,6)	1.3466	1.3546	1.3739	1.3754
R(5,19)	1.0729	1.0762	1.0864	1.0887
R(6,20)	1.0719	1.0751	1.0854	1.0877
R(7,10)	1.3874	1.3929	1.4036	1.4051
R(7,16)	1.0738	1.0771	1.0873	1.0895
R(8,9)	1.3874	1.3929	1.4036	1.4051
R(8,21)	1.0738	1.0771	1.0873	1.0895
R(9,10)	1.4245	1.4289	1.4491	1.4504
R(9,15)	1.4341	1.4358	1.4329	1.4344
R(10,11)	1.4341	1.4358	1.4329	1.4344
R(11,12)	1.0729	1.0762	1.0864	1.0887
R(11,13)	1.3466	1.3546	1.3739	1.3754
R(13,14)	1.4299	1.4312	1.4288	1.4306
R(13,22)	1.0719	1.0751	1.0854	1.0877
R(14,15)	1.3466	1.3546	1.3739	1.3754
R(14,23)	1.0719	1.0751	1.0854	1.0877
R(15,24)	1.0729	1.0762	1.0864	1.0887

Table 2: Optimized bond angles ($^{\circ}$) of anthracene molecule in different media.

Geometrical Parameter	RHF/6-31G		B3LYP/6-31	
	Gas	Ethanol	Gas	Ethanol
A(2,1,6)	120.5026	120.4908	120.4258	120.4711
A(2,1,17)	120.4399	120.384	120.2436	120.2384
A(6,1,17)	119.0574	119.1251	119.3307	119.2905
A(1,2,3)	120.9085	120.8532	120.9857	120.8877
A(1,2,18)	120.7818	120.7035	120.5779	120.6705
A(3,2,18)	118.3097	118.4433	118.4364	118.4419
A(2,3,4)	118.5889	118.656	118.5886	118.6413
A(2,3,7)	122.1413	122.0701	122.3186	122.1876
A(4,3,7)	119.2698	119.2739	119.0929	119.1712
A(3,4,5)	118.5889	118.6559	118.5885	118.6412

A(3,4,8)	119.2697	119.2743	119.0928	119.1712
A(5,4,8)	122.1413	122.0697	122.3187	122.1877
A(4,5,6)	120.9085	120.8532	120.9856	120.8876
A(4,5,19)	118.3097	118.4426	118.4364	118.4419
A(6,5,19)	120.7818	120.7042	120.578	120.6705
A(1,6,5)	120.5026	120.4909	120.4258	120.4712
A(1,6,20)	119.0577	119.1246	119.3313	119.2911
A(5,6,20)	120.4397	120.3846	120.2428	120.2377
A(3,7,10)	121.4606	121.4519	121.8144	121.6577
A(3,7,16)	119.27	119.2741	119.0931	119.1715
A(10,7,16)	119.2695	119.274	119.0925	119.1708
A(4,8,9)	121.4606	121.4518	121.8144	121.6577
A(4,8,21)	119.2699	119.2744	119.0932	119.1715
A(9,8,21)	119.2695	119.2738	119.0924	119.1708
A(8,9,10)	119.2697	119.2738	119.0928	119.1711
A(8,9,15)	122.1413	122.0698	122.3188	122.1878
A(10,9,15)	118.589	118.6563	118.5884	118.641
A(7,10,9)	119.2697	119.2741	119.0928	119.1711
A(7,10,11)	122.1413	122.0701	122.3186	122.1876
A(9,10,11)	118.589	118.6558	118.5887	118.6413
A(10,11,12)	118.31	118.4435	118.4365	118.442
A(10,11,13)	120.9084	120.8531	120.9856	120.8876
A(12,11,13)	120.7816	120.7034	120.5779	120.6704
A(11,13,14)	120.5026	120.4912	120.4257	120.471
A(11,13,22)	120.4396	120.3836	120.2432	120.238
A(14,13,22)	119.0578	119.1252	119.3311	119.2909
A(13,14,15)	120.5026	120.4903	120.4259	120.4713
A(13,14,23)	119.0578	119.1254	119.331	119.2908
A(15,14,23)	120.4396	120.3842	120.2431	120.2379
A(9,15,14)	120.9084	120.8533	120.9857	120.8877
A(9,15,24)	118.31	118.4431	118.4366	118.4421
A(14,15,24)	120.7816	120.7036	120.5777	120.6702

Table 3: Optimized Dihedral Angles ($^{\circ}$) of anthracene molecule in different media.

Geometrical Parameter	RHF/6-31		B3LYP/6-31	
	Gas	Ethanol	Gas	Ethanol
D(6,1,2,3)	0.0085	-0.0079	-0.0012	-0.0012
D(6,1,2,18)	-180.0102	180.0071	179.9981	179.9975
D(17,1,2,3)	180.008	-180.0052	179.9983	-180.0016
D(17,1,2,18)	-0.0107	0.0098	-0.0024	-0.0028
D(2,1,6,5)	-0.0012	0.0044	-0.0006	-0.0004
D(2,1,6,20)	-180.0069	180.0118	179.999	179.9994
D(17,1,6,5)	179.9993	-179.9982	179.9999	-180.0
D(17,1,6,20)	-0.0064	0.0091	-0.0005	-0.0002
D(1,2,3,4)	-0.0146	0.0106	0.0018	0.0008
D(1,2,3,7)	-180.0022	180.0091	-179.9971	180.0008
D(18,2,3,4)	-179.9963	-180.0041	-179.9974	-179.9979
D(18,2,3,7)	0.0161	-0.0056	0.0036	0.0021
D(2,3,4,5)	0.0134	-0.0097	-0.0007	0.001
D(2,3,4,8)	180.0085	-180.0018	-180.0006	-179.9978
D(7,3,4,5)	180.0013	-180.0082	179.9983	-179.999
D(7,3,4,8)	-0.0036	-0.0003	-0.0016	0.0022
D(2,3,7,10)	-180.0049	179.9991	179.9994	179.9983

D(2,3,7,16)	-0.0098	0.0043	-0.0014	-0.0024
D(4,3,7,10)	0.0077	-0.0024	0.0004	-0.0017
D(4,3,7,16)	180.0027	180.0028	179.9996	179.9976
D(3,4,5,6)	-0.0065	0.0065	-0.001	-0.0025
D(3,4,5,19)	-180.0023	179.9998	179.9993	179.9987
D(8,4,5,6)	179.9985	179.9984	179.9988	179.9962
D(8,4,5,19)	0.0027	-0.0083	-0.0009	-0.0026
D(3,4,8,9)	-0.0014	-0.0002	0.0012	-0.0007
D(3,4,8,21)	180.0084	-180.0062	-179.9976	180.0006
D(5,4,8,9)	-180.0065	180.008	-179.9986	180.0006
D(5,4,8,21)	0.0033	0.002	0.0026	0.0018
D(4,5,6,1)	0.0003	-0.0037	0.0017	0.0022
D(4,5,6,20)	180.006	-180.0111	-179.9979	-179.9975
D(19,5,6,1)	-180.004	180.0032	-179.9986	180.001
D(19,5,6,20)	0.0017	-0.0042	0.0018	0.0012
D(3,7,10,9)	-0.0066	0.0055	0.0011	-0.0003
D(3,7,10,11)	-179.9986	179.9992	-179.9985	180.0001
D(16,7,10,9)	-180.0016	-179.9997	-179.9981	180.0004
D(16,7,10,11)	0.0063	-0.0059	0.0022	0.0008
D(4,8,9,10)	0.0025	0.0033	0.0003	-0.0013
D(4,8,9,15)	180.005	-180.0032	180.0003	179.9987
D(21,8,9,10)	-180.0073	180.0092	179.9991	179.9974
D(21,8,9,15)	-0.0047	0.0028	-0.0009	-0.0025
D(8,9,10,7)	0.0015	-0.0059	-0.0014	0.0018
D(8,9,10,11)	-180.0062	-179.9998	179.9982	-179.9985
D(15,9,10,7)	-180.001	-179.9996	-180.0014	-179.9982
D(15,9,10,11)	-0.0087	0.0064	-0.0018	0.0014
D(8,9,15,14)	180.0028	180.0016	-179.9984	179.9995
D(8,9,15,24)	0.0036	0.0028	0.0024	0.0009
D(10,9,15,14)	0.0053	-0.0048	0.0016	-0.0005
D(10,9,15,24)	180.0062	-180.0036	-179.9976	180.001
D(7,10,11,12)	-0.0047	0.0083	0.0014	-0.0001
D(7,10,11,13)	180.0034	-179.9974	-180.0001	179.9976
D(9,10,11,12)	180.0032	180.0021	-179.9983	180.0003
D(9,10,11,13)	0.0113	-0.0036	0.0003	-0.002
D(10,11,13,14)	-0.0101	-0.001	0.0014	0.0016
D(10,11,13,22)	-180.006	179.9995	-180.0002	-179.9999
D(12,11,13,14)	-180.0018	-180.0068	180.0	179.9992
D(12,11,13,22)	0.0023	-0.0063	-0.0017	-0.0022
D(11,13,14,15)	0.0064	0.0028	-0.0017	-0.0006
D(11,13,14,23)	180.0012	180.0049	-180.0004	-179.9996
D(22,13,14,15)	180.0024	-179.9978	179.9999	-179.9991
D(22,13,14,23)	-0.0028	0.0044	0.0012	0.0019
D(13,14,15,9)	-0.0039	0.0002	0.0002	0.0
D(13,14,15,24)	-180.0048	-180.001	179.9993	179.9986
D(23,14,15,9)	180.0013	-180.0019	-180.0011	-180.001
D(23,14,15,24)	0.0004	-0.0032	-0.002	-0.0024

Table 4: Dipole moments (in Debye) in gas phase and ethanol obtained using RHF and B3LYP methods.

RHF/6-31G		B3LYP/6-31	
Gas	Ethanol	Gas	Ethanol
0.0003	0.0003	0.0000	0.0000

Table 5: Quadrupole moments(in Debye) in gas phase and ethanol.

RHF/6-31G			B3LYP/6-31G		
Gas			Ethanol		
XX	YY	ZZ	XX	YY	ZZ
-69.4309	-70.0816	-91.7071	-66.8135	-67.8178	-89.9211
Gas			Ethanol		
XX	YY	ZZ	XX	YY	ZZ
-70.2391	-70.9301	-86.5803	-66.5629	-67.8575	-86.9452

Table 6: Predicted thermal energies (kcal/mol) in gas phase and ethanol for anthracene molecule obtained using RHF and B3LYP methods.

Energy	RHF/6-31G		B3LYP/6-31G	
	Gas	Ethanol	Gas	Ethanol
Total Energy	137.058	134.846	129.172	128.283
Electronic Energy	0.000	0.000	0.000	0.000
Translational Energy	0.889	0.889	0.889	0.889
Rotational Energy	0.889	0.889	0.889	0.889
Vibrational Energy	135.281	133.069	127.395	126.506

Table 7: Electrostatic potential derived charges on different atomic positions of anthracene molecule in gas phase and ethanol.

S/N	Atom	RHF/6-31G		B3LYP/6-31G	
		Gas	Ethanol	Gas	Ethanol
1	C	-0.099099	-0.086073	-0.070869	-0.087024
2	C	-0.273560	-0.284203	-0.211148	-0.237186
3	C	0.231306	0.242868	0.196931	0.203503
4	C	0.231306	0.233456	0.196931	0.194860
5	C	-0.273561	-0.272865	-0.211150	-0.226797
6	C	-0.099098	-0.099706	-0.070868	-0.099200
7	C	-0.517887	-0.533159	-0.401578	-0.443229
8	C	-0.517887	-0.531535	-0.401578	-0.441837
9	C	0.231304	0.239461	0.196930	0.208845
10	C	0.231304	0.235328	0.196930	0.204879
11	C	-0.273559	-0.274940	-0.211148	-0.235444
12	H	0.156788	0.153876	0.112495	0.133509
13	C	-0.099100	-0.094367	-0.070869	-0.069005
14	C	-0.099100	-0.091341	-0.070868	-0.066114
15	C	-0.273559	-0.279741	-0.211149	-0.240018
16	H	0.240497	0.248847	0.170733	0.199296
17	H	0.123261	0.118999	0.088015	0.091468
18	H	0.156788	0.155712	0.112494	0.129855
19	H	0.156788	0.153936	0.112495	0.128184
20	H	0.123261	0.121830	0.088015	0.093957
21	H	0.240497	0.248328	0.170732	0.198881
22	H	0.123261	0.120323	0.088015	0.112196
23	H	0.123261	0.120020	0.088015	0.111909
24	H	0.156788	0.154947	0.112495	0.134511

Table 8: Polarizabilities of anthracene using RHF and B3LYP methods.

orientation	RHF/6-31G		B3LYP/6-31G	
	Gas	Ethanol	Gas	Ethanol
xx	230.248	346.355	265.371	382.047
xy	0.000	0.004	0.000	0.004
yy	136.995	226.380	149.437	227.444
xz	0.000	0.032	0.000	0.027
yz	0.001	-0.023	0.000	-0.008
zz	30.674	47.748	40.085	48.630

3.4. Vibrational frequencies and assignments

The vibrational spectrum of a molecule is considered to be a unique physical property and is characteristic of the molecule. As such, the infrared (IR) spectrum can be used as a fingerprint for identification by the comparison of the spectrum from an 'unknown' with previously recorded reference spectra. The fundamental requirement for infrared activity, leading to absorption of infrared radiation, is that there must be a net change in dipole moment during the vibration for the molecule or the functional group under study. The vibrational frequency is usually expressed in cm^{-1} [5]. Another important form of vibrational spectroscopy is Raman spectroscopy, which is complementary to infrared spectroscopy. The selection rules for Raman spectroscopy are different to those for infrared spectroscopy, and in this case a net change in bond polarizability must be observed for a transition to be Raman active [6].

In this work, Gaussian software was used to predict the vibrational spectra of anthracene molecule in its ground state. These frequency calculations are valid only at stationary points on the potential energy surface, thus our computations were performed on the optimized structures of the molecules. As 6-31G is the smallest basis set that gives satisfactory results for frequency calculations, it was used. Raw frequency calculations computed at the Hartree-Fock level contain known systematic errors due to the neglect of electron correlation, resulting to overestimates of about 10-12%. Therefore, it is usual to scale frequencies predicted at the HF level by an empirical factor of 0.8929. Use of this factor has been demonstrated to produce very good agreement

with experiment for a wide range of systems. Our values in this study must be expected to deviate even a bit more from experiment because of the choice of a medium-sized basis set (6-31G)- around 15%. For B3LYP/6-31G a scale factor of 0.9613 is used [4].

Some IR and Raman intense vibrational frequencies and their approximate descriptions for the molecule in gas phase and ethanol at RHF and B3LYP levels with 6-31G basis set are presented in Tables 9-12. The frequencies reported are not scaled as is usually done in comparing the similar calculated frequency with observed frequency (as no experimental results were found for the comparison). The B3LYP results show a significant lowering of the magnitudes of the calculated frequencies.

The most intense IR vibrational frequency for anthracene at RHF level in gas phase is 844.793cm^{-1} (718.636 cm^{-1} in ethanol) corresponding to C-H symmetric stretching of the benzene rings (Table 9), while the most intense Raman vibrational frequency is 1534.75 cm^{-1} (1549.21 cm^{-1} in solution) corresponding to benzene ring distortions (Table 11). At B3LYP level of theory, the most intense IR vibrational frequency is 3221.85 cm^{-1} in gas phase (3060.08 cm^{-1} in ethanol) corresponding to C-H anti-symmetric stretching of the ring in plane (Table 10) and the most intense Raman vibrational frequency is 3222.5 cm^{-1} (3060.44 cm^{-1} in ethanol) corresponding to C-H symmetric stretching of the benzene rings (Table 12).

The various IR and Raman spectra for the molecule at different levels of theory and in different media are shown in Figs. 2-5.

Table 9: Some IR intense vibrational frequencies and their approximate description for anthracene molecule at RHF/6-31G level of theory.

S/N	Gas	Ethanol	Approximate Description
1	536.672	454.48	C-H symmetric stretching of the rings in plane
2	680.343	582.824	C-C anti-symmetric stretching of the rings
3	844.793	718.636	C-H symmetric stretching of the rings and C-C-H angle bending
4	1058.48	952.081	C-H stretching of the middle ring
5	1819.65	1817.41	C-C anti-symmetric stretching of the rings
6	3367.25	3090.64	C-H anti-symmetric stretching of the rings
7	3381.79	3102.85	C-H symmetric stretching of the rings

Table 10: Some IR intense vibrational frequencies and their approximate description for anthracene molecule at B3LYP/6-31G level of theory.

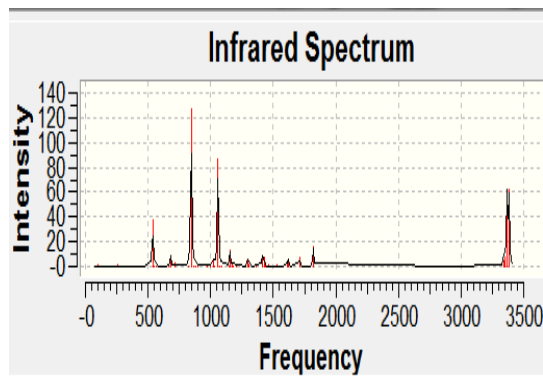
S/N	Gas	Ethanol	Approximate Description
1	760.28	820.3	C-H symmetric stretching of the rings in plane
2	920.096	965.578	C-H symmetric stretching of the rings out of plane
3	3206.92	3048.47	C-H anti-symmetric stretching of the rings in plane
4	3221.85	3060.08	C-H anti-symmetric stretching of the rings in plane

Table 11: Some Raman intense vibrational frequencies and their approximate description for anthracene molecule at RHF/6-31G level of theory.

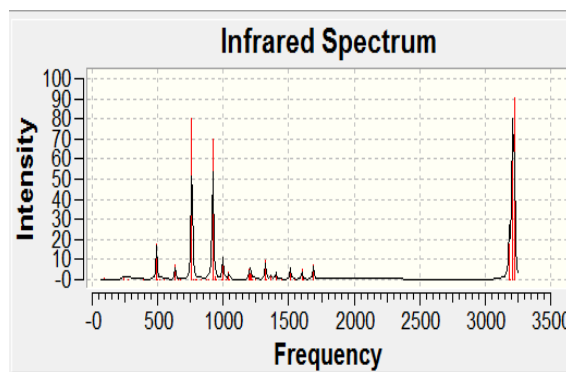
S/N	Gas	Ethanol	Approximate Description
1	430.483	425.675	C-C symmetric stretching of the rings in plane
2	596.25	594.42	C-C anti-symmetric stretching of the rings in plane
3	823.928	824.174	rings breathing
4	894.233	910.791	C-H symmetric stretching of the rings
5	1073.84	1109.59	C-C symmetric stretching of the rings and C-C-H bending
6	1340	1337.08	C-H anti-symmetric stretching of the rings
7	1364.2	1356.32	C-C anti- symmetric stretching of the rings
8	1534.75	1549.21	Ring distortions
9	1730.87	1664.54	C-H anti-symmetric stretching of rings
10	3352.08	3080.47	C-H symmetric stretching of rings
11	3366.85	3090.09	C-H anti-symmetric stretching of rings
12	3382.38	3103.29	C-H symmetric stretching of rings

Table 12: Some Raman intense vibrational frequencies and their approximate description for anthracene molecule at B3LYP/6-31G level of theory.

S/N	Gas	Ethanol	Approximate Description
1	773	406.261	C-C symmetric stretching of the rings
2	1047.39	1059.73	C-C anti-symmetric stretching of the rings
3	1451.19	1262.3	Ring distortions
4	1543.41	1332.25	C-C anti-symmetric stretching of the rings
5	1610.48	1499.21	Ring distortions
6	3192.13	3037.5	C-H symmetric stretching of the rings
7	3206.62	3048.18	C-H anti- symmetric stretching of the rings
8	3222.5	3060.44	C-H symmetric stretching of the rings

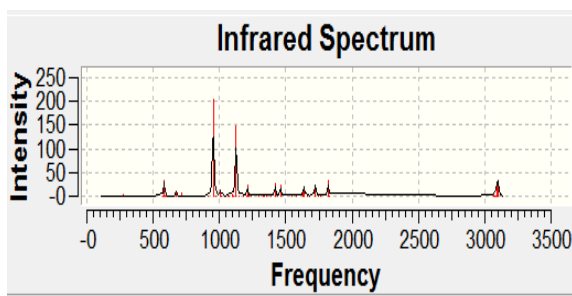


(a) RHF

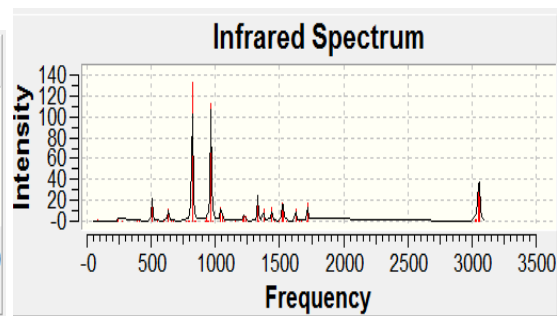


(b) B3LYP

Fig.2: IR spectrum for anthracene in gas phase.

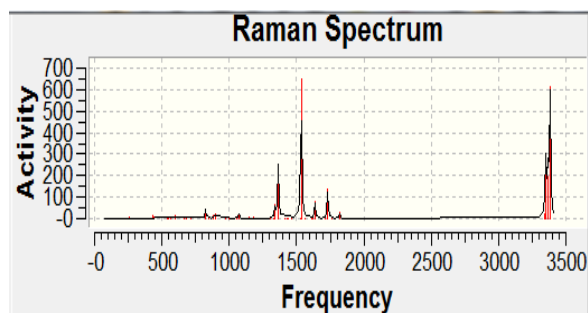


(a) RHF

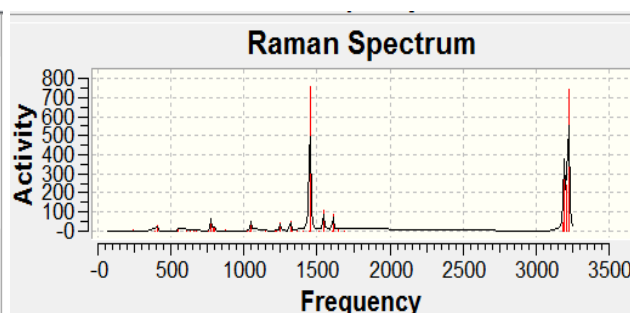


(b) B3LYP

Fig.3: IR spectrum for anthracene in ethanol.



(a) RHF



(b) B3LYP

Fig.4: Raman spectrum for anthracene in gas phase.

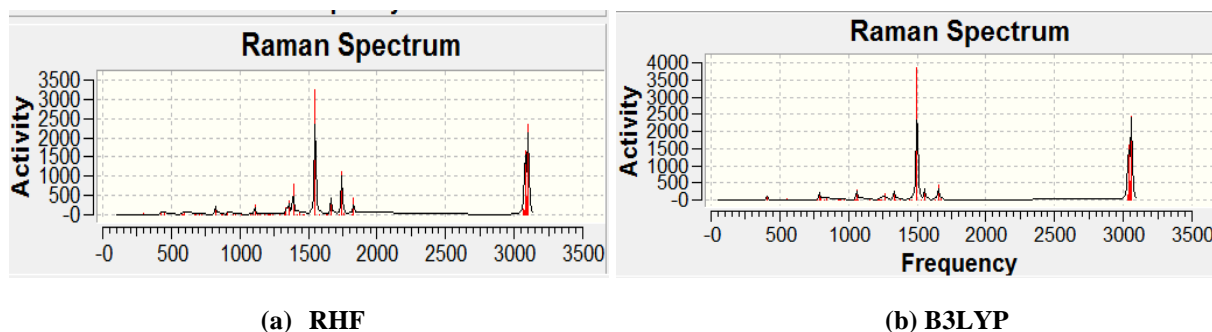


Fig.5: Raman spectrum for anthracene in ethanol.

4. Conclusion

The practicability of our findings in this work is an encouraging factor. This work has exposed the molecular and electronic properties of anthracene for use in the fabrication of organic semi conductor devices.

To compliment this research work, the experimental part of this study can be undertaken to ascertain the accuracy of this computational technique. Also, this work can be done using other computational physics softwares and results compared with our results in this work. Anthracene can be studied in other environments to see the effect of these environments on their physical properties. Other solvents that can be considered include hexane, benzene, hydronaphthalenes, Carbon disulfide, Chloroform, and other organic solvents.

Acknowledgments

We are thankful to the Council of Scientific and Industrial Research (CSIR), India for financial support through the Emeritus Professor scheme (Grant No. 21(0582)/03/EMR-II) to Prof. A. N. Singh of the Physics Department, Bahamas Hindu University, India, which enabled him to purchase the Gaussian software. We are most grateful to Emeritus Prof. A. N. Singh for donating this software to the Physics Department, Gombe State University, Nigeria.

References

- [1] W. James, *Product Engineering: Molecular Structure and Properties* (Oxford University Press, 2007).
- [2] D. M. Kimberly and M. Ernest, Prokopchuk J. Chem. Educ. **88**(8), 1155-(2011).
- [3] A. D. Becke, J. Chem. Phys. **98**, 5648 (1993).
- [4] Gaussian 03, Revision C.02, 2004, M. J. Frisch, G. W. Trucks, H. B. Schlegel, G. E. Scuseria, M. A. Robb, J. R. Cheeseman, J. A. Montgomery, T. Vreven Jr., K. N. Kudin, J. C. Burant, M. Millam, S. S. Iyengar, J. Tomasi, V. Barone, B. Mennucci, M. Cossi, G. Scalmani, N. Rega, G. A. Petersson, H. Nakatsuji, M. Hada, M. Ehara, K. Toyota, R. Fukuda, J. Hasegawa, M. Ishida, T. Nakajima, Y. Honda, O. Kitao, H. Nakai, M. Klene, X. Li, J. E. Knox, H. P. Hratchian, J. B. Cross, C. Adamo, J. Jaramillo, R. Gomperts, R. E. Stratmann, O. Yazyev, A. J. Austin, R. Cammi, C. Pomelli, J. W. Ochterski, P. Y. Ayala, K. Morokuma, G. A. Voth, P. Salvador, J. J. Dannenberg, V. G. Zakrzewski, S. Dapprich, A. D. Danniels, M. C. Strain, O. Farkas, D. K. Malick, A. D. Rabuck, K. Raghavachari, J. B. Foresman, J. V. Ortiz, Q. Cui, A. G. Baboul, S. Clifford, J. Cioslowski, B. B. Stefanov, G. Liu, A. Liashenko, P. Piskorz, I. Komaromi, R. L. Martin, D. J. Fox, T. Keith, M. A. Al-Laham, C. Y. Peng, A. Nanayakkara, M. Challacombe, P. M. W. Gill, B. Johnson, W. Chen, M. W. Wong, C. Gonzalez and J. A. Pople, Gaussian, Inc., Wallingford CT (2004).
- [5] C. Lee, W. Yang and R. G. Parr, Phys. Rev. B **37**, 785 (1988).
- [6] J. Coates, "Interpretation of Infrared Spectra, A Practical Approach" in *Encyclopedia of Analytical Chemistry*, Ed. R. A. Meyers (John Wiley & Sons, Chichester, 2000) p.10815.

Received: 21 May, 2012

Accepted: 26 June, 2012